


Low-temperature densification of ceramics and cermets by the intermediary stage activated sintering method

Thomaz Augusto Guisard Restivo^{1,2,3}  · Michelangelo Durazzo³ ·
Sonia Regina Homem de Mello-Castanho³ · Ana Cugler Moreira¹ ·
Sergio Graciano¹ · Victor Bridi Telles² · Jorge Alberto Soares Tenorio²

Received: 24 September 2016 / Accepted: 29 June 2017
© Akadémiai Kiadó, Budapest, Hungary 2017

Abstract The article explores new concepts in order to promote ceramic and cermet materials sintering at lower temperatures between 1200 and 1300 °C. The principle of the new process method called intermediary stage activated sintering (ISAS) involves the preparation of the ceramic powder with dispersed doping agents, such as nanotubes and fibers, which shape the pore structure at pressed pellets with stable interconnected thin cylinders between the grains. This feature resembles and extends the condition found during the intermediary stage sintering, which enhances the ions diffusion rate along tubular pores to increase shrinkage. Carbon nanotubes (CNT) and nanofibers are homogenized into cubic zirconia and alumina in amounts ranging from 1 to 10 vol% at high-energy milling devices and ultrasound disruptor under ethanol media. Ni, Cu and Mo/MoO₃ can be also added to provide tubular channel filling. Sintering of uniaxially pressed pellets is carried out in a dilatometer and tubular furnaces at 1200/1300 °C under air, argon and controlled oxygen partial pressure atmospheres. TG/DTA/MS analyses of sample pellets reveal the oxidation and gas release temperature and duration. The results demonstrate the ISAS process concept is valid since it further increases the ceramic final density by 8% of the theoretical density at 1200 °C, leading to close the porosity at 1300 °C,

compared to 1500–1600 °C temperatures at conventional process. Short CNT and cellulose nanofiber were found to be the best additives in this sense.

Keywords Sintering · Carbon nanotube · Carbon fiber · Cermets · Dilatometry

Introduction

Ceramic and cermet are distinguishing materials that exhibit advanced and combined properties for structural and functional components. The fabrication processes for such materials often require high-temperature sintering steps at 1600 °C or above, demanding costly gas burning furnaces or sophisticated electric heating elements. The present article explores new concepts in order to develop novel processes to promote sintering. The first approach is based on authors' patent [1], where the so-called process sintering by activated surface—SAS, is detailed. The evolution of SAS process gives rise to the present new method: intermediary stage activated sintering—ISAS. Both researches aim to reach powder formulations allied to processing parameters in order to reduce the sintering temperature down to the range 1200–1300 °C, where Ni–Cr low-cost furnaces can be employed.

The sintering by activated surface (SAS) concept derives primary from a low-temperature densification method employed for UO₂ based on the retraction of the U ions diameter due to changes of oxidation states from +4 to +5 driven by CO₂ atmospheres. In this way, U diffusion coefficient increases by several magnification orders [2, 3]. Similarly, when applied to other ceramic materials, SAS process can explore the effects of partial oxidation to promote sintering. Moreover, SAS process

✉ Thomaz Augusto Guisard Restivo
guisard@dglnet.com.br

¹ University of Sorocaba UNISO, Sorocaba, SP 18023000, Brazil

² Department of Chemical Engineering, Polytechnics of Sao Paulo USP, São Paulo, SP 05424970, Brazil

³ IPEN, Institute of Energetic and Nuclear Research, São Paulo, SP 05508000, Brazil

makes use of thin metallic adherent films of selected additives over the ceramic particles in order to preserve their surface area. High-energy milling (mechanical alloying—MA) powder preparation technique has been employed for obtaining thin metallic coating over the ceramic particles. During MA processing, microforging impacts lead to metal flattening and coating the ceramic particles [4–6]. The particle coating method is actually an extension of the macroscopic mechanical plating process [7] down to micro- and nanosize scale. In this sense, metal layers are expected to cover and block ceramic surface defects to prevent surface diffusion phenomena, thereby preserving the original powder surface area. The additives selection holds choosing metals and oxides that decompose or evaporate along the heating cycle in the range 600–1200 °C, being this feature another specific highlight of the method. At such temperatures, these metal films are displaced, revealing active surfaces that can promptly sinter. The candidates for volatile additives successfully employed are Mo, Ag and Cu. Under oxidizing atmospheres, the first metal reacts to MoO₃ that melts at 802 °C and evaporates over 1100 °C. By its turn, Ag and Cu melt at 907 and 1085 °C, respectively, being also volatiles over 1100 °C. Thus, these oxide/metallic films act as sacrificial layers, being inert regarding to ceramic phase, and provide an effective protection to the particle surfaces while allowing the rearrangement of particles after melting. Indeed, high-energy milling is a way to force the contact between the powder constituents, leading to layered powder morphologies [8]. Such powder and aggregate morphologies have more suitable geometries to allow wetting of the ceramic particles by molten films and to withdraw the volatile gases through channels along the green pellet. Besides the evaporation process, the particle surfaces approach due to capillarity forces. The effect is likely to occur when the vapor pressure of the film is about 50 Pa at the sintering temperature, say, when the evaporation rate is slow. The authors have demonstrated the efficiency of the SAS method to lower sintering temperatures of zirconia cermets with 40 vol% metallic additives, for instance solid oxide fuel cell (SOFC) anodes with superior catalytic activities [8, 9]. Afterward, the method was applied to zirconia with lower content of metal doping.

The extension of the research based on SAS technique led to other variants shown presently: ceramic sintering with carbon fibers and nanotubes dopants. The method herein shown comprises doping ceramics with carbon fibers and carbon nanotubes (CNT). The conceived principle is based on pore shaping where carbon fibers or nanotubes are oxidized to CO₂ under controlled oxygen partial pressure, leaving cylindrical pores in their places. Such very small pores can introduce new defects rather

than increasing the porosity itself, thereby promoting the diffusion. Accordingly to the accepted sintering theory [10], the objective is to extend the second (intermediary) stage of sintering, where the pores are cylindrical and the densification is fast, while delaying the third (final) stage and to avoid the formation of isolate pores. Carbon fibers [11] and CNT [12, 13] have been extensively investigated as reinforce oxides and other ceramics for improving mechanical properties, including SiC and some commercial materials. Prepared composites are said to have superior fracture toughness, approaching the ultimate theoretical strength. The composites often show limited uses at high temperatures due to decomposition, transformation and reaction of fiber compound. Milsom et al. [14] have prepared partially stabilized zirconia containing 3 mol% yttria doped with 2 vol% of multiwalled CNT and sintered the samples at spark plasma sintering equipment (SPS), concluding that CNT is a good sintering aid due to the formation of a network for easy diffusion of cations. The sintering process did not oxidize the CNT, which has been burned during post-treatment of sample, meaning there was a reducing sintering atmosphere in SPS die. Some authors have reported doping agents up to 2 mol% can lower the sintering temperature of tetragonal and cubic zirconia, such as Fe, Co and Mn, added as calcined nitrates [15, 16]. However, the preparation of anode-supported NiO–YSZ/YSZ SOFC half-cell required a 1350 °C co-sintering step for obtaining a dense electrolyte.

Experimental

The starting commercial ceramic powders were cubic 8 mol% yttria-stabilized zirconia (YSZ), 13 m² g⁻¹, $d(50) = 0.3 \mu\text{m}$, from Tosoh Corp. and CT-3000 alumina, 7.8 m² g⁻¹, $d(50) = 0.6 \mu\text{m}$ from Almatris. Metallic Ni, Mo and Cu powders $d(50) = 5 \mu\text{m}$ were obtained from Aldrich, while the silver powder from Ticon with 99.5% purity has mean particle size of 20 μm . Four types of carbon materials were employed: two types of MWCNT (multiwalled carbon nanotubes $\phi < 8 \text{ nm}$) short SCNT (2–5 μm) and conventional CNT (10–30 μm), a 40-nm-diameter CNT (CNT40) and a 12 k carbon fiber (CF) with individual diameter of about 7 μm . The carbon fiber strips were cut and dispersed in the high-energy milling device for 5 min at PTFE vial and $\phi 5\text{-mm}$ zirconia spheres rated to powder at 50:1 by mass. After milling, the material was sieved at 45 μm to remove the fines. CNT dispersion in ceramic powders is important to assure detangling of the nanotubes, which has been accomplished often by ultrasonification under different media, including ethanol, during 1–2 h [17–19]. Some

authors employ planetary milling to complement the dispersion [20, 21]. In the present work, carbon materials and fiber were first treated in 100 W ultrasonic bath and mixed with YSZ/alumina powder in ethanol media and submitted to high-power ultrasound disruptor (500 W) with Ti tip for 3–40 min. A 3 mass% dispersion of cellulose nanofiber in water was used to prepare the respective doped ceramic powders. In other experimental sets, high-energy milling (MA) was carried out at a 19 Hz shaker mill with lined vial and spheres made from tetragonal zirconia (YTZ), even dry or under ethanol. The last method was employed for longer times to prepare Ni-, Cu- and Mo-doped zirconia powders. In some cases, the YTZ lining was not used to reduce pulverizing the nanotubes and fibers. The ball to powder mass ratio employed was 10:1–50:1. All powders were sieved through 200 μm after milled and dried. Sample pellets were pressed from 100 to 300 MPa load into $\phi 8\text{-mm}$ die. SAS and ISAS processes were finally combined: Zirconia powder was first high-energy milled for 1 h with Ni and Cu powders and subsequently submitted to ultrasound for CNT dispersion. Geometric densities were determined while the percent of theoretical densities were computed by simple sum law, assuming there are no reactions between the constituents. The resulting green densities were in the range 48–62% TD. The SAS process was carried out at a tubular furnace with heating rate of 10 $^{\circ}\text{C min}^{-1}$ up to 1200 $^{\circ}\text{C}$ for 3 h under argon flow (100 mL min^{-1}), controlling the oxygen partial pressure through two different ways: equilibrium estimative for water vapor decomposition and flowmeters. ISAS process was carried out in a vertical furnace under air. Some pellets were also sintered at a dilatometer and TG/DSC (Setaram Setsys 1750 $^{\circ}\text{C}$) up to 1200 and 1300 $^{\circ}\text{C}$ under Ar and synthetic air controlled by flowmeter, where PO_2 was set at 10^{-2} , approximately (Ar: 50 mL min^{-1} ; air: 3 mL min^{-1}). In further dilatometric experiments, air flows of 1 and 25 mL min^{-1} were adjusted. The probe load was set at 2 g to avoid any influence on retraction. TG/DSC/MS analysis was also performed to study carbon and metal oxidation during heating to sintering temperature. Sintered samples were analyzed at SEM-FEG/EDS.

The identification of samples follows the scheme:

$CER_xDOP_tMt_Py$, where:

CER : YSZ or AIO: cubic yttria-stabilized zirconia or alumina;

$xDOP$: x is the amount in vol% of carbon nanotube type, carbon fiber (CF) or cellulose fiber (FCel) doping and/or metal doping;

tM or Mt : preparing method, MA (mechanical alloying) or US (ultrasound); t the processing time in minutes or hours (if specified);

Py : ultrasound power y % of 500 W.

Results and discussion

The MA and US-processed powders were easily pressed into sound pellets owing to high homogeneity and lubricant action when doped with carbon materials. Zirconia powder is rather inert, but alumina shows limited reaction with some carbon additives (CF and CNT) during 1200 $^{\circ}\text{C}$ sintering. As a result, the pellets often deform.

SAS method

MA is employed in the present work either for long period milling and microforging to render metal plating on the ceramic particles or for dispersion during shorter times. The first technique gives some typical powder morphologies of YSZ–metal cermets as shown in Fig. 1: plated round ceramic particles or incrustated, layered particles and aggregates.

Silver and Mo doping in YSZ powders has a different behavior on densification (Fig. 2) as a function of PO_2 (a) and composition (b). The Ag-bearing powders were sintered to high densities under inert atmospheres with low oxygen partial pressure, with maximum density at 10 vol% Ag. Cu-doped zirconia shows high density as well. Conversely, low content Mo powders shrink under air. The results for these powders suggest SAS process is running by melting metallic Ag as well as oxidizing Mo to MoO_3 , which melts and sweeps out through the pores. The vapor pressure level of Ag (about 25 Pa at 1200 $^{\circ}\text{C}$) [22] is in the proper range to cause slow evaporation during sintering process. However, MoO_3 evaporation would be faster since its vapor pressure is close to 1000 Pa at the melting point (802 $^{\circ}\text{C}$). Nevertheless, the delay of Mo metal oxidation during heating can lower such vapor volume to reasonable values, allowing SAS process.

ISAS method

One first set of samples doped with 10 vol% CNT prepared by MA was analyzed by dilatometry at heating rate of 10 $^{\circ}\text{C min}^{-1}$ up to 1200 and 1300 $^{\circ}\text{C}$. The oxidation of carbon must be slow to allow enough time to sweep out the gas from the pores. Hence, it was imposed oxygen partial pressure of 10^{-2} with argon in the dilatometer, starting from the beginning of the 1200 $^{\circ}\text{C}$ isotherm. Figure 3 shows that if the green density is excessive and the oxygen total flow (air) is insufficient to oxidize C before sintering starts, the pellet swells. It is interesting to note this occurs even far before the closing pores condition, being dependent of the gas flow, C content and heating period. When the air flow is established since the beginning of the analysis, the swelling is not observed.

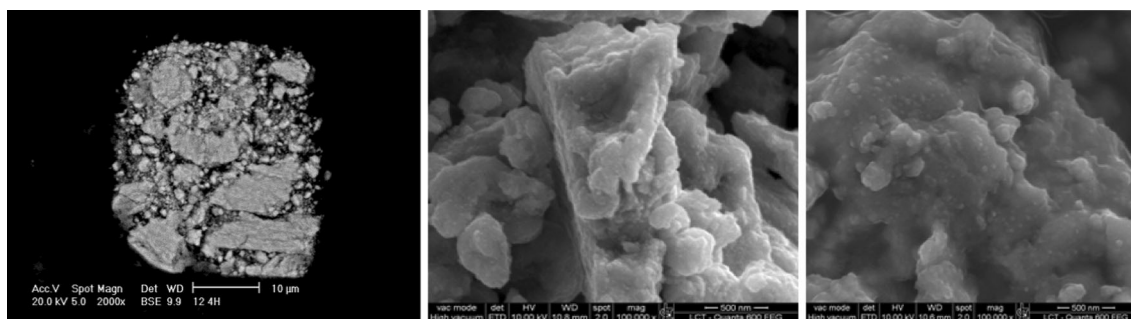


Fig. 1 Typical powder morphologies of MA for long periods: *left* YSZ-Ni; at *center*: wafer-type morphology of YSZ-Ni-Cu-Mo; at *right*: embedded ceramic particles YSZ-Ni-Cu-Mo

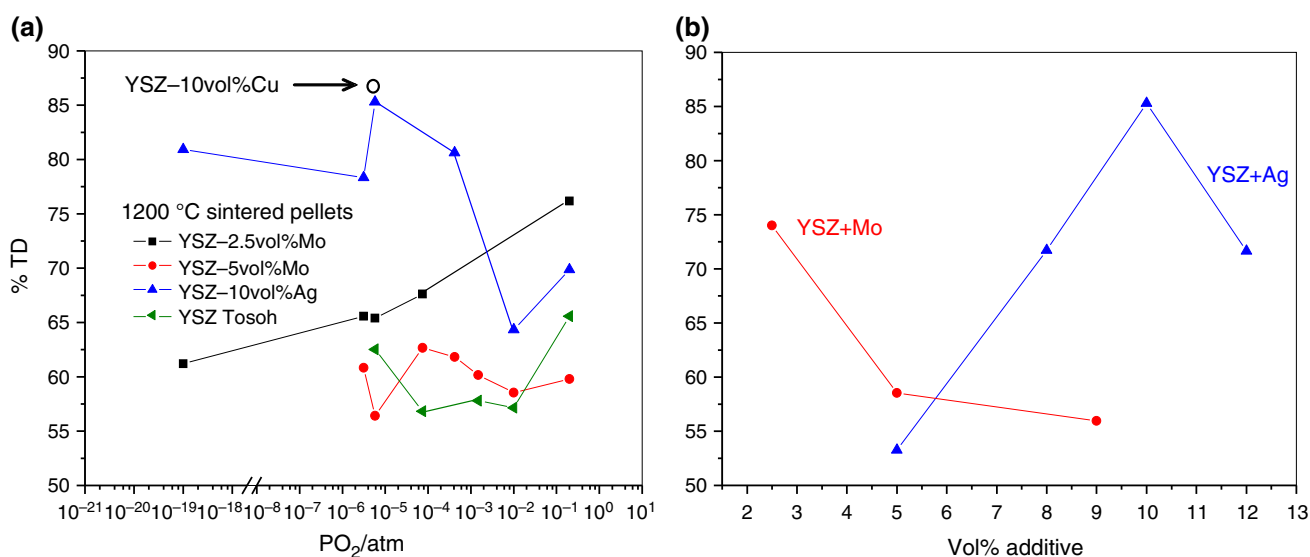


Fig. 2 Sintering behavior of Ag- and Mo-doped YSZ as a function of PO_2 (a) and composition (b)

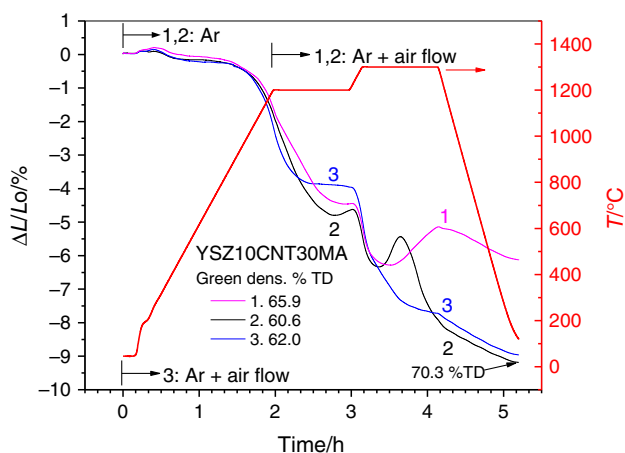


Fig. 3 Sintering behavior by dilatometry of CNT-doped YSZ with different green densities and atmospheres

Carbon fiber of 7 μm diameter was observed in SEM together with some milled YSZ-CNT and YSZ-CF powders to check their dispersion in zirconia. Figure 4 shows

the carbon fiber and CNT were pulverized or strongly deformed after 30-min MA, while they can be found as numerous of rather dispersed broken pieces through the powder with 5-min MA. CNT has shown a similar behavior at milling (Fig. 4), in spite it should be stronger and far smaller (25–50 nm diameter). A less strong milling under ethanol media and 10:1 ball to powder ratio avoids the CNT pulverizing and gives rather good homogenization (Fig. 5). However, even in this condition, 20 min appears to be excessive since the CNT is hardly found.

Figure 6 compares different processing variants with respect to dry milling time and carbon content. The heating cycle at $10^\circ C\ min^{-1}$ heating rates includes 1200 and $1300^\circ C$ isotherms. In general, the shorter is the MA duration the higher is the shrinkage and final density. Pulverizing of the tube/fibers structure is deleterious to the under-development sintering process, as it has been conceived. Carbon fiber seems to be less efficient to promote sintering than CNT. Alumina-doped powder also shrinks

Fig. 4 *Left* carbon fiber upper to down: original fiber, 5 and 30 min MA; *right* upper do down: CNT as received, 5- and 30-min MA

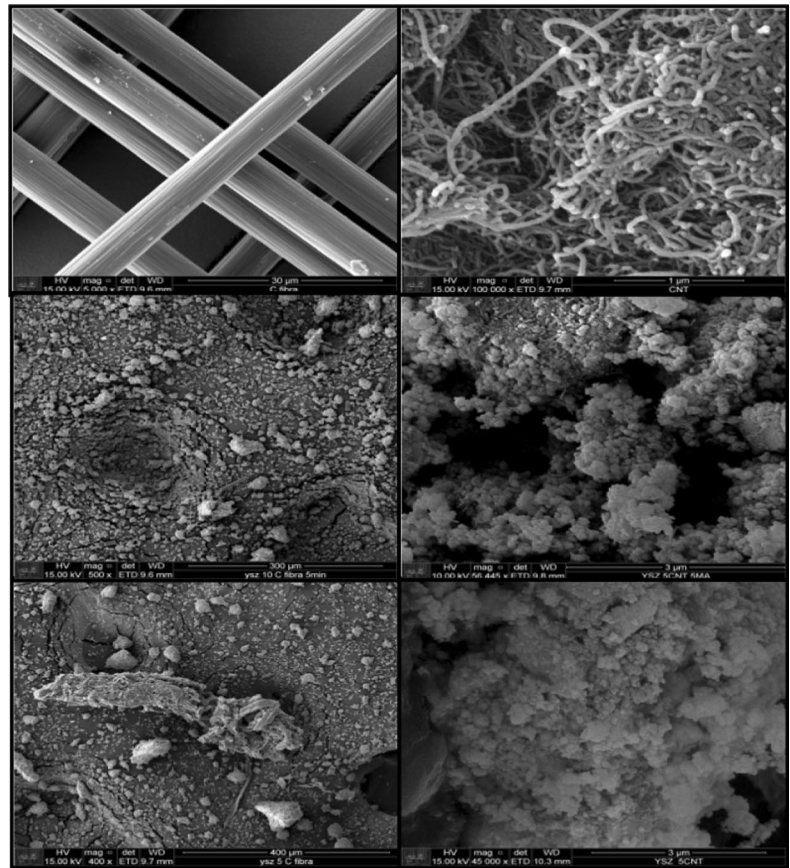
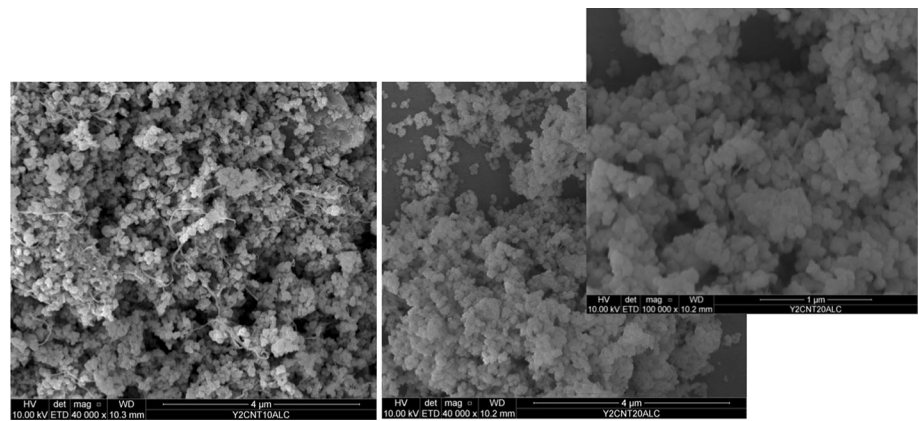


Fig. 5 SEM micrographs of YSZ/CNT-milled sample under ethanol during 10 min (*left*) and 20 min (*right/up*)



less than zirconia, which is more active due to smaller particle size and greater surface area.

Pellets sintering behavior comparison between pure YSZ and YSZ-CNT doped and milled under ethanol for 10 min is shown in Fig. 7. The dilatometric curves reveal the CNT doping and milling under alcohol is very efficient in increasing the density at 1200 °C sintering by 6% linear retraction.

Better results were obtained with powder ultrasonification (US) in ethanol media. Some features for CNT and FCl are shown in Fig. 8 for fractured green pellets. There is a tendency to alignment of nanofibers and CNT orthogonally to compact direction. The additives are well dispersed by the ultrasound action.

The sintering behavior of ISAS-processed powders was first investigated for different CNT types and CF doping in

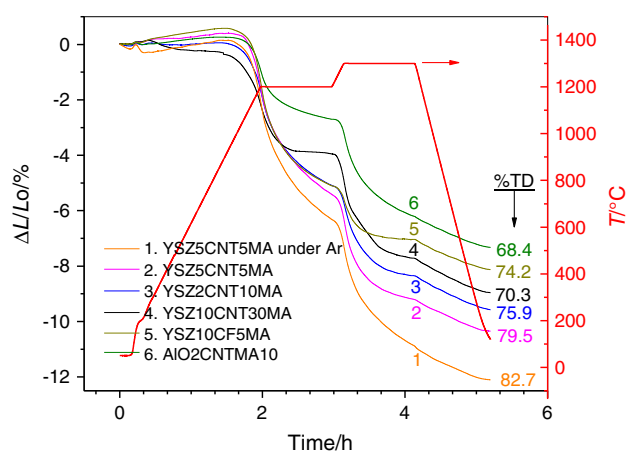


Fig. 6 Sintering at various conditions under Ar + 5% air (pure Ar at sample 1), including the final density; green densities varied from 57 to 59% DT; and sample 2: 62% DT

various amounts at 1200 °C/3 h heating in a vertical furnace. Figure 9 groups the results where it can be noted the short SCNT 8-nm nanotube at 2 vol% provides the best results of final density. Since most part of materials has shown higher sintered density for 2 vol% of additives, this amount was considered for further analysis.

Fig. 7 Comparison for shrinkage of pure and doped zirconia by dilatometry: 10 °C min⁻¹ up to 400/1 h and 1300 °C/3 h isotherms

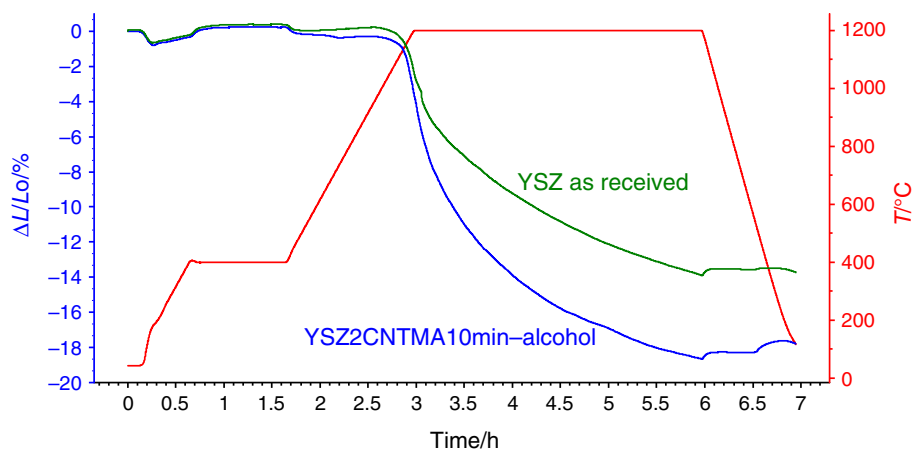


Figure 10 compares the densification of zirconia as received and doped with SCNT and FCEl at 1200 and 1300 °C where the final density increases about 7% for doped materials. Zirconia treated by US for 40 min is also included to demonstrate the ultrasound is irrelevant to activate non-doped YSZ powders. One can note the onset sintering temperature was anticipated from 1000 to 900 °C. These combined results strongly support the new ISAS hypothesis.

Once the shrinkage profiles can be influenced by the heating cycle, a straight 1300 °C sintering study was performed, as seen in Fig. 11. The as-received YSZ results are denser at 1300 °C (87.9% TD) while 2 vol% of additives has increased the density to high values up to 95.6% TD. All SCNT-doped zirconia powders reach high density without cracks, meaning the additive is very effective to promote sintering, no matter are their initial green densities. Sample YSZ2SCNTUS3 has shown an expansion from 450 to 790 °C which indicates CO₂ has encountered some difficulty to sweep out from pores. The SCNT doping in alumina does not seem to promote sintering in the same conditions (73.1% TD), where the temperature level was insufficient for this material.

Cermets containing Ni and Cu at amounts of 0.5 vol% doped with 2 vol% CNT and cellulose nanofiber (FCEl)

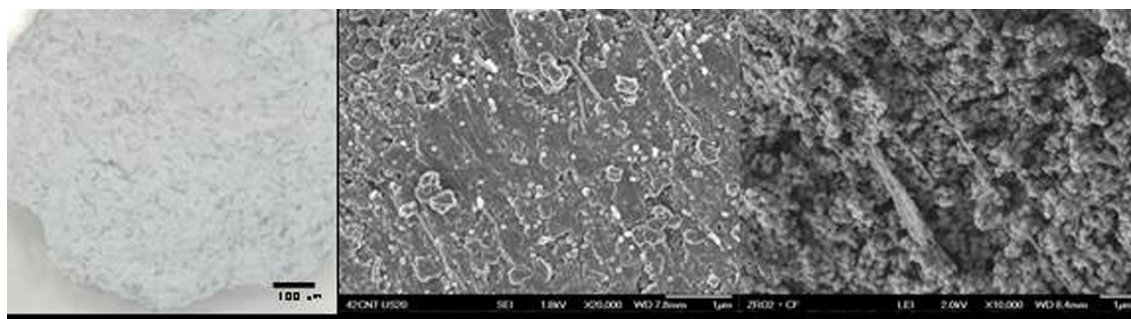


Fig. 8 Dispersion of fractured pellets: left YSZ2CFUS30 (optical); center YSZ2CNTUS20; and right YSZ2FCElUS5

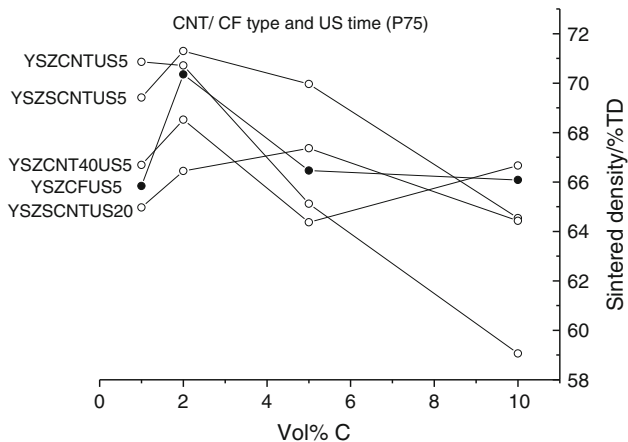


Fig. 9 Comparison between different CNT/CF doping on zirconia sintering at 1200 °C/3 h, under air

show interesting results in the sense these powders attain high green density due to metal content, reaching 62% DT. Therefore, the shrinkage is smaller but it can still reach high density, as shown in Fig. 12. The retraction profiles of Ni-bearing cermets are identical which means the SCNT has minor effect on shrinkage. Copper-doped cermet shrinks more slowly at the beginning but still retracts after 3 h at 1300 °C, indicating it could reach high density for longer times. Ni doping shows attractive interaction regarding carbon, which can be dissolved in the metal lattice, while Cu, inversely, repels C [9] and can even form liquid phase at sintering temperature to drive the shrinkage.

Final density of sintered pellets at 1200 and 1300 °C for 3 h is grouped in Table 1. The results analysis indicates that both Fcel and SCNT additives rated at 2 vol%

Fig. 10 Sintering behavior for doped, US-treated and as-received YSZ; initial green densities from 46 to 49% TD

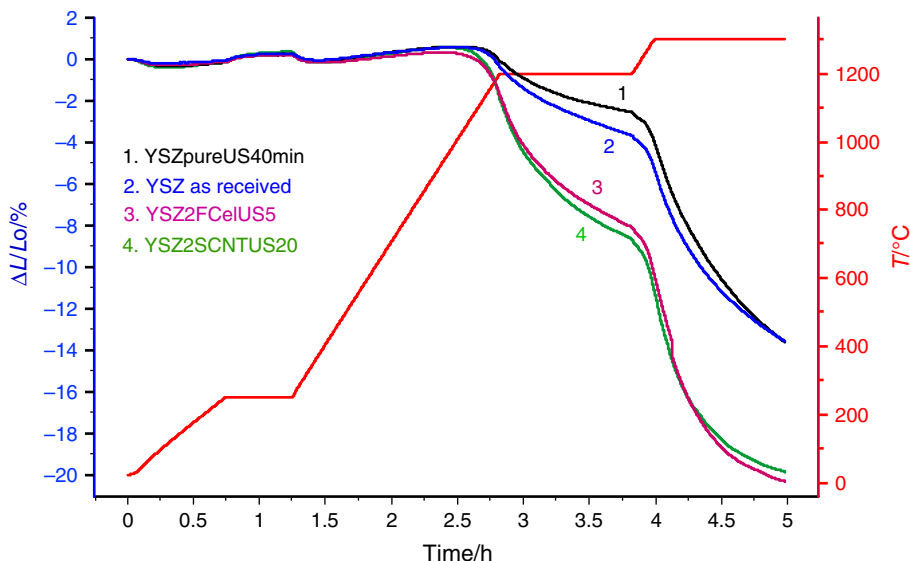


Fig. 11 Compilation of 1300 °C sintering by dilatometry; heating rate 10 °C min⁻¹, 1 mL min⁻¹ air flow

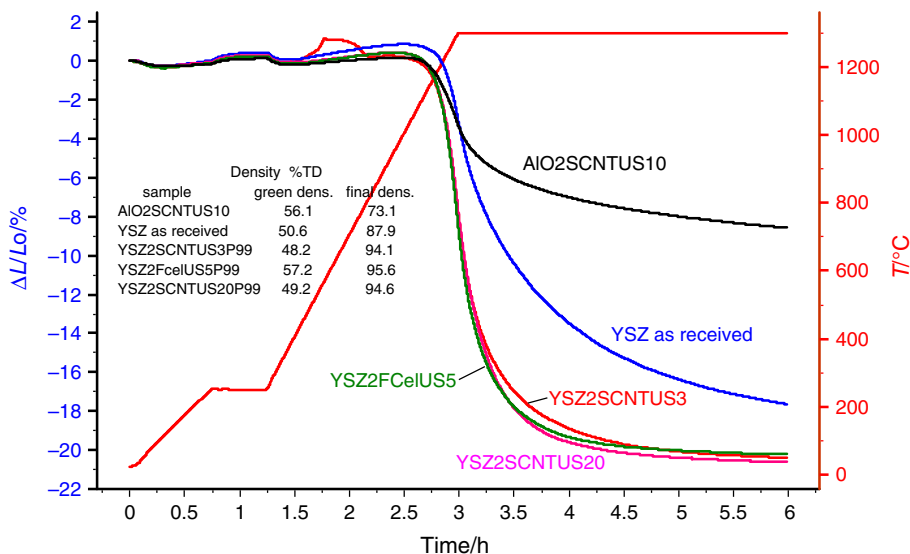
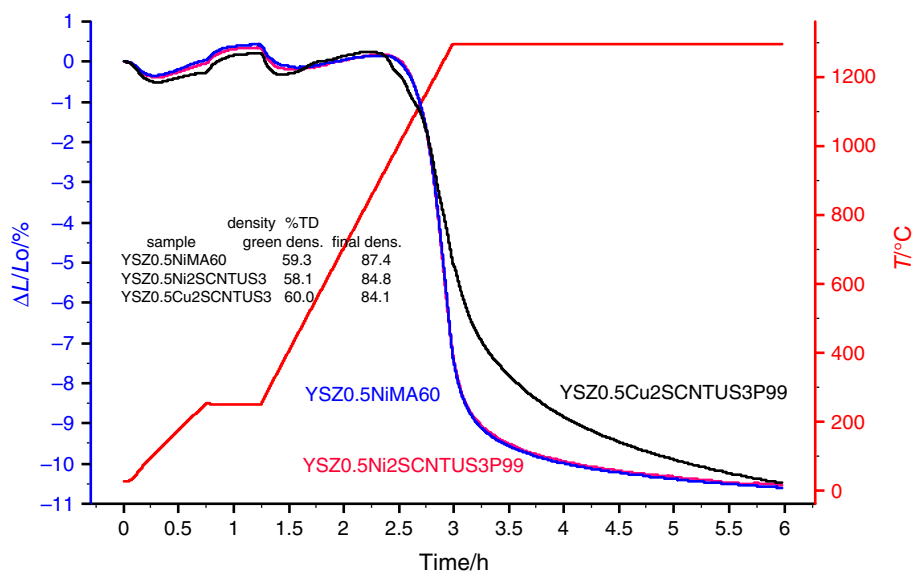


Fig. 12 Sintering behavior of Ni-, Cu- and SCNT-doped zirconia; heating rate $10\text{ }^{\circ}\text{C min}^{-1}$, 1 mL min^{-1} air flow



promote sintering to 95% TD and increase the density by more than 7% TD, while CF is less effective. CNT-doped and non-doped (Ni, Cu) cermet densify somewhat less, but one must consider the green density can be still increased by pressing at higher loads allowed by the cermet. Highly sintered samples often show mass loss of $-1, 8\%$ after sintering, suggesting this is the right volume of gas that can be swept out from the compact body to assure the correct balance between sintering promotion and pore forming or swelling. Besides the ISAS theory, where carbon materials feature provide channeling tubes for diffusion likewise the intermediary sintering stage, admixing high surface area materials (i.e., SCNT: $\text{BET} = 500\text{ m}^2\text{ g}^{-1}$) to the ceramic plays an important role on promoting the densification.

The oxidation of carbon additives during the sintering cycle was further investigated by TG/DSC/MS monitoring the ion current related to CO_2 and O_2 (Fig. 13). The TG/DSC/MS results show the evolution of the oxidation product CO_2 occurs in two phases: The first CO_2 step release starts at about $200\text{ }^{\circ}\text{C}$ up to $550\text{ }^{\circ}\text{C}$, and the second takes place at higher temperatures, from 850 to $1150\text{ }^{\circ}\text{C}$. These surprising results indicate the nanofibers and especially the nanotubes do not undergo total oxidation into the pellet core, but rather there is some diffusion delay of oxygen into the pores. Corresponding DSC exothermic peaks and mass losses are aligned to small O_2 signal drops at the curves. The temperature of oxidation phases varies for different additives: anticipates for FCell and also somewhat for Ni/Cu-bearing cermets. The last cermets seem to further prevent the second step of SCNT oxidation, especially for Cu-added cermet. Copper repeals C and may favor C

dispersion and reactivity by increasing its availability. The combined CNT and FC pellet YSZ1SCNT1CFUS5P99 shows two carbon-burning peaks: The second corresponding to CF oxidation, which is less active than SCNT. According to XRD analysis for sintered CNT-doped YSZ

Table 1 ISAS sintering results at 1200 and $1300\text{ }^{\circ}\text{C}$ for 3 h , $10\text{ }^{\circ}\text{C min}^{-1}$ heating rate

Sample	Sintering $T/^{\circ}\text{C}$	$\Delta m/\text{\%mass}$	Green dens./ \%TD	Sint. dens./ \%TD
YSZ2SCNTUS3P99	1200	-1.60	47.54	72.77
YSZ2SCNTUS5P75		-2.40	46.80	71.29
YSZ1CNTUS5P75		-1.52	48.66	70.86
YSZ1.5CNTMA15 min		-2.17	44.98	70.16
YSZ5SCNT		-2.86	47.47	69.96
Y2SCNT20USP75		-1.20	47.02	69.58
YSZ as received		-1.26	46.86	66.69
YSZ2FCeIUS5P99	1300	-1.79	57.22	95.59
YSZ2SCNTUS20P75		-1.80	49.19	94.59
YSZ2SCNTUS3P99		-1.80	48.18	94.08
YSZ0.5CuMA60 min		-1.76	48.56	92.77
YSZ0.5NiMA60 min		-1.79	47.97	91.63
YSZ2SCNTUS3P99		-1.98	43.61	89.73
YSZ2SCNTUS20P75		-1.71	45.41	89.56
YSZ2CNTUS5P75		-1.90	44.62	88.42
YSZ as received		-0.55	50.64	87.87
YSZ2CFUS3P99		-1.10	48.93	87.00
Y0.5Ni2SCNTUS3P99		-1.74	60.86	86.67

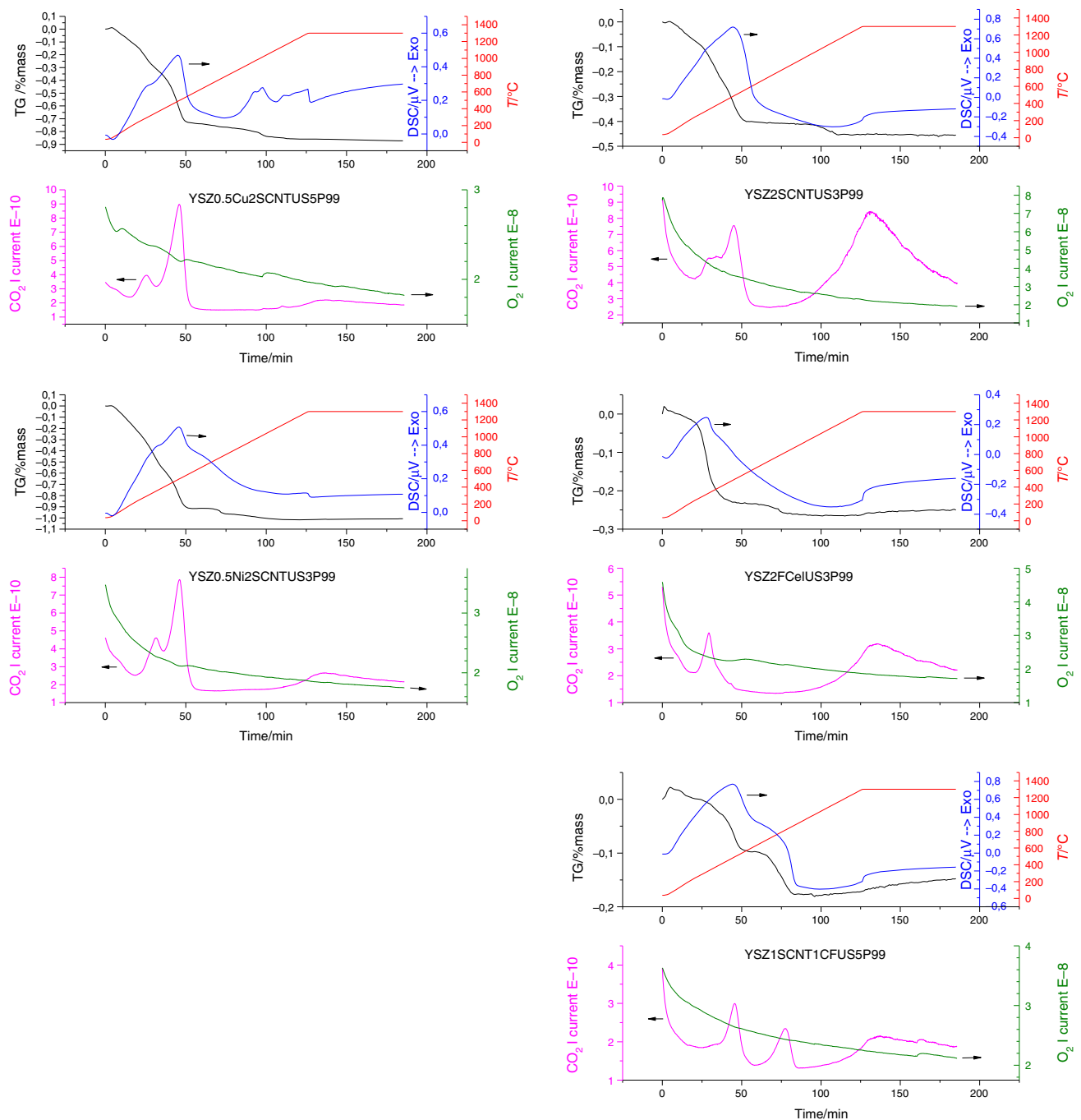


Fig. 13 TG/DSC/MS analysis of zirconia doped with different additives up to 1300 °C at 10 °C min⁻¹ heating rate

at 1300 °C, there is no change in reflections profile regarding the original cubic yttria–zirconia, since it is a very stable compound.

Sintered microstructures for SAS/ISAS show high density at periphery while some porosity remains in the pellet

core for YSZ–10Ag (Fig. 14). In the case of YSZ-2 vol% SCNT, the material is rather dense after 1300 °C/3 h sintering, except by some few pore regions, which can be compared to many pores at sintered YSZ without doping additives.

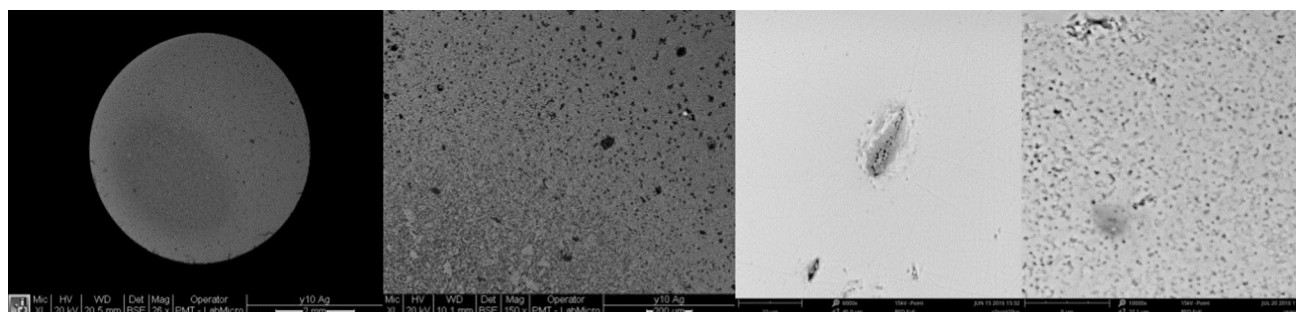


Fig. 14 Sintered microstructures (left to right): 1200 °C-sintered YSZ10Ag with porous core; detail of YSZ10Ag; dense YSZ2SCNTUS5P75 sintered at 1300 °C; and pure YSZ (1300 °C) showing numerous small pores for comparison

Conclusions

SAS process gathers some parallel techniques to enable low-temperature sintering centered on protecting ceramic powder surface area before trigger sintering. ISAS poro-shaping approach by carbon nanotube, nanofibers and carbon fiber is also effective if good dispersion is obtained, regarding their morphology is conserved during the preparation methods. The main drawback of SAS/ISAS technique is the sweeping out of gases that may form as a result of evaporation or reaction of additives. Since CNT is an expensive additive, the author has equally demonstrated that doping with nanofiber shapes, for instance, cellulose nanofiber, can lead to excellent results when employing careful preparation methods. The present results demonstrated the SAS process can increase the 1200 °C sintering zirconia pellet density from about 65% TD up to 87% TD, while ISAS can lead to 83% TD. The densification is virtually full at 1300 °C, reaching 96% TD with gains over 7% TD. Besides CNT, Ni and Cu additives are advantageous in order to increase the green density as a strategy to densify in lower temperatures, together with the presence of some liquid phase and volatile compounds. In both processes, preparation and sintering methods must be carefully adjusted.

Acknowledgements Funding was provided by FAPESP (Grant No. 2014/211220) and CNPq (Grant No. 150672/2012-8).

References

- Mello-Castanho SRH, Restivo TAG. Processo de sinterização por superfície ativada para a densificação de corpos compósitos cerâmicos e metálicos em baixas temperaturas. BR Patent PI 1105476-0, INPI. 11/11/2011.
- Assmann H, Dörr W, Peehs M. Control of UO₂ microstructure by oxidative sintering. *J Nucl Mater.* 1986;140:1–6.
- Hj Matzke. Diffusion-processes in nuclear-fuels. *J Less-Common Met.* 1986;121:537–64.
- Restivo TAG, Mello-Castanho SRH. Nickel–Zirconia cermet processing by mechanical alloying for solid oxide fuel cell anodes. *J Power Sources.* 2008;185:1262–6.
- Restivo TAG, Mello-Castanho SRH. YZrO₂–Ni cermet processing by high energy milling. *Mater Sci Forum.* 2008;591–593:514–20.
- Guisard Restivo TA, Mello-Castanho SRH. Cu–Ni–YSZ anodes for solid oxide fuel cell by mechanical alloying processing. *Int J Mater Res.* 2010;101:128–32.
- Wood WG. *Metals handbook (ASM handbook). Surface cleaning, finishing, and coating, vol. 5.* 9th ed. Metals Parks: ASM International; 1982. p. 300–3.
- Restivo TAG, Mello-Castanho SRH. Sintering studies on Ni–Cu–YSZ SOFC anode cermet processed by mechanical alloying. *J Therm Anal Calorim.* 2009;97:775–80.
- Restivo TAG, Mello-Castanho SRH, Tenorio JAS. TG/DTA–MS evaluation of methane cracking and coking on doped nickel–zirconia based cermets. *J Therm Anal Calorim.* 2014;118(1):75–81.
- Rahaman MN. *Ceramic processing and sintering.* 2nd ed. Boca Raton: CRC Press; 2003. p. 482.
- Davidge RW. Fibre-reinforced ceramics. *Composites.* 1987;18(2): 92–8.
- Aguilar-Elguézabal A, Bocanegra-Bernal MH. Fracture behaviour of α -Al₂O₃ ceramics reinforced with a mixture of single-wall and multi-wall carbon nanotubes. *Compos B.* 2014;60:463–70.
- Zapata-Solvas E, Gómez-García D, Domínguez-Rodríguez A. Towards physical properties tailoring of carbon nanotubes-reinforced ceramic matrix composites. *J Eur Ceram Soc.* 2012; 32(12):3001–20.
- Milsom B, et al. The effect of carbon nanotubes on the sintering behaviour of zirconia. *J Eur Ceram Soc.* 2012;32:4149–56.
- Dey T, et al. Transition metal-doped yttria stabilized zirconia for low temperature processing of planar anode-supported solid oxide fuel cell. *J Alloys Compd.* 2014;604:151–6.
- Guo F, Xiao P. Effect of Fe₂O₃ doping on sintering of yttria-stabilized zirconia. *J Eur Ceram Soc.* 2012;32:4157–64.
- Bocanegra-Bernal MH, et al. A comparison of the effects of multi-wall and single-wall carbon nanotube additions on the properties of zirconia toughened alumina composites. *Carbon.* 2011;49:1599–607.
- Taheri M, et al. High/room temperature mechanical properties of 3Y-TZP/CNTs composites. *Ceram Int.* 2014;40:3347–52.
- Guo-Dong Zhan, et al. Single-wall carbon nanotubes as attractive toughening agents in alumina-based nanocomposites. *Nat Mater.* 2003;2:38–42.
- Yamamoto G, et al. Microstructure-property relationships in pressureless-sintered carbon nanotube/alumina composites. *Mater Sci Eng A Struct.* 2014;617:179–86.
- Sudhakar C, et al. Preparation of carbon nanotube doped ceramic powders for plasma spraying using heterocoagulation method. *J Eur Ceram Soc.* 2015;35:989–1000.
- Alcock CB, Kubaschewski O, Spencer PJ. *Materials thermochemistry. International series on materials science and technology.* 6th ed. Oxford: Pergamon Press; 1993.